

---

This is an electronic reprint of the original article.  
This reprint may differ from the original in pagination and typographic detail.

Wester, Niklas; Mynttinen, Elsi; Etula, Jarkko; Lilius, Tuomas; Kalso, Eija; Kauppinen, Esko I.; Laurila, Tomi; Koskinen, Jari

**Simultaneous Detection of Morphine and Codeine in the Presence of Ascorbic Acid and Uric Acid and in Human Plasma at Nafion Single-Walled Carbon Nanotube Thin-Film Electrode**

*Published in:*  
ACS Omega

*DOI:*  
[10.1021/acsomega.9b02147](https://doi.org/10.1021/acsomega.9b02147)

Published: 01/01/2019

*Document Version*  
Publisher's PDF, also known as Version of record

*Published under the following license:*  
CC BY-NC-ND

*Please cite the original version:*  
Wester, N., Mynttinen, E., Etula, J., Lilius, T., Kalso, E., Kauppinen, E. I., Laurila, T., & Koskinen, J. (2019). Simultaneous Detection of Morphine and Codeine in the Presence of Ascorbic Acid and Uric Acid and in Human Plasma at Nafion Single-Walled Carbon Nanotube Thin-Film Electrode. *ACS Omega*, 17726-17734. <https://doi.org/10.1021/acsomega.9b02147>

---

This material is protected by copyright and other intellectual property rights, and duplication or sale of all or part of any of the repository collections is not permitted, except that material may be duplicated by you for your research use or educational purposes in electronic or print form. You must obtain permission for any other use. Electronic or print copies may not be offered, whether for sale or otherwise to anyone who is not an authorised user.

# Simultaneous Detection of Morphine and Codeine in the Presence of Ascorbic Acid and Uric Acid and in Human Plasma at Nafion Single-Walled Carbon Nanotube Thin-Film Electrode

Niklas Wester,<sup>\*,†</sup> Elsi Mynttinen,<sup>‡</sup> Jarkko Etula,<sup>†</sup> Tuomas Lilius,<sup>§,||</sup> Eija Kalso,<sup>§,⊥</sup> Esko I. Kauppinen,<sup>#</sup> Tomi Laurila,<sup>‡</sup> and Jari Koskinen<sup>†</sup>

<sup>†</sup>Department of Chemistry and Materials Science, Aalto University, Kemistintie 1, 02150 Espoo, Finland

<sup>‡</sup>Department of Electrical Engineering and Automation, Aalto University, Tietotie 3, 02150 Espoo, Finland

<sup>§</sup>Department of Pharmacology, University of Helsinki, Haartmaninkatu 8, 00290 Helsinki, Finland

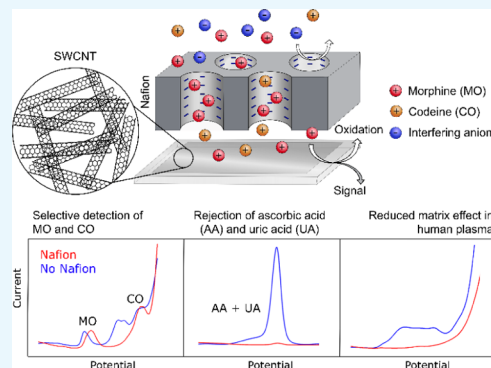
<sup>||</sup>Department of Clinical Pharmacology, University of Helsinki and Helsinki University Hospital, Tukholmankatu 8C, 00290 Helsinki, Finland

<sup>⊥</sup>Pain Clinic, Department of Anesthesiology, Intensive Care and Pain Medicine, University of Helsinki and Helsinki University Hospital, Haartmaninkatu 2A, 00290 Helsinki, Finland

<sup>#</sup>Department of Applied Physics, Aalto University School of Science, P.O. Box 15100, FI-00076 Aalto, Finland

## Supporting Information

**ABSTRACT:** In clinical settings, the dosing and differential diagnosis of the poisoning of morphine (MO) and codeine (CO) is challenging due to interindividual variations in metabolism. However, direct electrochemical detection of these analytes from biological matrices is inherently challenging due to interference from large concentrations of anions, such as ascorbic acid (AA) and uric acid (UA), as well as fouling of the electrode by proteins. In this work, a disposable Nafion-coated single-walled carbon nanotube network (SWCNT) electrode was developed. We show facile electron transfer and efficient charge separation between the interfering anions and positively charged MO and CO, as well as significantly reduced matrix effect in human plasma. The Nafion coating alters the voltammetric response of MO and CO, enabling simultaneous detection. With this SWCNT/Nafion electrode, two linear ranges of 0.05–1 and 1–10  $\mu\text{M}$  were found for MO and one linear range of 0.1–50  $\mu\text{M}$  for CO. Moreover, the selective and simultaneous detection of MO and CO was achieved in large excess of AA and UA, as well as, for the first time, in unprocessed human plasma. The favorable properties of this electrode enabled measurements in plasma with only mild dilution and without the precipitation of proteins.



## 1. INTRODUCTION

Morphine (MO) and codeine (CO) are alkaloids from the opioid drug class that are widely used in pain management.<sup>1</sup> The use of morphine and codeine is, however, associated with adverse effects, such as nausea, vomiting, constipation, sedation, dependence, and respiratory depression.<sup>2</sup> MO is a strong opioid used to treat moderate and severe postoperative as well as cancer pain, whereas the weak opioid codeine is used as an antitussive and analgesic to treat moderate pain. Unlike morphine, codeine is considered a prodrug and is metabolically activated by *O*-demethylation to morphine.

The biotransformation of codeine to morphine is mediated by the genetically polymorphic enzyme cytochrome P450 (CYP) 2D6. Interindividual differences in CYP2D6 activity cause significant variation in the efficacy and safety of codeine as an analgesic. Poor metabolizers lacking CYP2D6 activity have been shown to have extremely low plasma morphine concentrations and therefore no analgesic effect.<sup>3</sup> On the other

hand, several cases of severe side effects have been reported after the intake of codeine in individuals later identified as ultrarapid metabolizers of CYP2D6 substrates.<sup>4–6</sup> In addition, significant variation in the bioavailability of oral morphine has been reported.<sup>7</sup> Morphine is also one of the main active metabolites of heroin, and the morphine/codeine ratio in blood has been proposed as a biomarker for heroin abuse.<sup>8</sup> Thus, a fast, inexpensive method for determining the individual concentrations of these opioids in the presence of each other is highly desirable.

Current methods require a dedicated laboratory and personnel, as well as time-consuming sample processing. In contrast, electrochemical measurements are relatively rapid,

Received: July 11, 2019

Accepted: October 2, 2019

Published: October 16, 2019

mobile, and inexpensive. Moreover, the electrochemical detection of drugs in biological matrices has been reported.<sup>9–11</sup>

In recent years, single-walled carbon nanotubes (SWCNTs) have attracted a great deal of attention due to their unique structure and extraordinary properties, such as large surface area, mechanical strength, high electrical conductivity, and electrocatalytic activity.<sup>12</sup> By means of aerosol chemical vapor deposition, large areas of porous SWCNT electrodes with high conductivity and surface area can be produced.<sup>13,14</sup> This process allows for the collection of patterned networks that can be easily press-transferred to produce electrodes without the need for the modification of conventional carbon electrodes.<sup>13–15</sup> This enables the production of inexpensive disposable SWCNT electrodes.

Unfortunately, biological fluids always contain high concentrations (100–500  $\mu\text{M}$ ) of electroactive interferents such as ascorbic acid (AA) and uric acid (UA).<sup>16</sup> In contrast, therapeutic plasma morphine concentrations usually range between 10 and 100 nM.<sup>3,17,18</sup> However, concentrations above 1  $\mu\text{M}$  have been reported in patients with advanced cancer and in fatal cases of morphine poisoning.<sup>19,20</sup> Similarly, physiologically relevant concentrations of codeine range from approximately 100 to 400 nM,<sup>3,21</sup> and postmortem concentrations around 1  $\mu\text{M}$  have been reported.<sup>8</sup> Nonetheless, achieving sufficient selectivity is challenging due to the large difference in these concentrations and overlapping voltammetric peaks, especially of UA and MO.

To overcome this issue, biological matrices are often considerably diluted and spiked with the target analytes.<sup>9–11</sup> Another strategy is to coat the electrode with a permselective membrane.<sup>9,22–25</sup> Nafion is a sulfonated copolymer that has been used extensively due to its antifouling and cation exchange properties to increase selectivity and long-term signal stability in electrochemical measurements.<sup>23,26</sup> Since both AA and UA exist as anions under physiological conditions, their interference can be significantly reduced by a Nafion membrane, as shown in numerous studies.<sup>9,23–25</sup> Moreover, the similar structures of MO and CO cause MO peaks to overlap with CO peaks at carbon electrodes.<sup>27–29</sup> However, we have recently shown that combining a tetrahedral amorphous carbon (ta-C) electrode with a recast Nafion membrane can not only virtually eliminate the interference of AA and UA but also increase the selectivity by eliminating some of the peaks observed for the opioids with the same functionalities.<sup>9</sup> Similarly, a Nafion membrane has also been shown to alter the detection of morphine by decreasing the number of peaks observed.<sup>30</sup>

While the detection of morphine<sup>23,29,31–33</sup> and codeine<sup>34,35</sup> has been reported by several groups, only a few groups have reported the simultaneous detection of MO and CO.<sup>10,36–38</sup> Even fewer reports can be found on direct and selective electrochemical detection of MO and CO in the presence of large excess of both AA and UA.<sup>38</sup> Moreover, to the best of our knowledge, the simultaneous detection of MO and CO has not been reported with SWCNT or Nafion/SWCNT electrodes. In this paper, we combine the novel SWCNT network and a Nafion membrane as a dual-layer electrochemical sensor to achieve the selective detection of MO and CO. The clinical applicability of the sensor is also evaluated by demonstrating the simultaneous detection of MO and CO in the presence of large excess of AA and UA, as well as in human plasma.

## 2. RESULTS AND DISCUSSION

**2.1. Characterization.** Figure 1A shows the cross-sectional scanning electron microscopy (SEM) image of the Nafion/

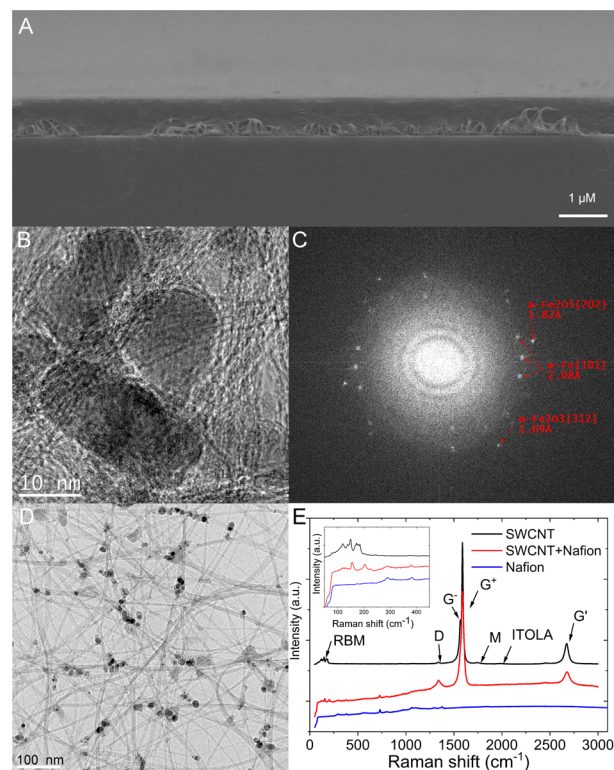


**Figure 1.** Characterization of the Nafion/SWCNT electrode. (A) SEM cross-sectional image of Nafion/SWCNT electrode, (B) HRTEM image of typical iron nanoparticles, (C) fast Fourier transform of the HRTEM image of typical iron nanoparticles, (D) TEM image of the SWCNT network, and (E) Raman spectra of the SWCNT, Nafion/SWCNT, and Nafion-coated glass slide. The inset in (E) shows the radial breathing mode (RBM) region for all samples.

SWCNT electrode. The thickness of the coating was analyzed from 121 SEM images over the full cross section. An average thickness of  $1.2 \pm 0.5 \mu\text{m}$  was found. Because prior X-ray photoelectron spectroscopy (XPS) measurements were unable to reliably detect iron, the SWCNT network was studied further with transmission electron microscopy (TEM) and energy-dispersive spectroscopy (EDS). Figure 1B shows a typical high-resolution TEM (HRTEM) image of the iron nanoparticles embedded in the SWCNT network. A lower-magnification TEM image of the SWCNT network is shown in Figure 1D, where the iron nanoparticles appear dark. Fast Fourier transform analysis reveals *d*-spacings attributed to both metallic iron and likely iron oxides, shown and assigned in Figure 1C. This assignment was confirmed with EDS analysis that revealed the presence of C, O, Fe, K, Si, and S (Supporting Information Table S1). Cu was also found, likely originating from the TEM grid.

Figure 1E shows the Raman spectra of the SWCNT, Nafion/SWCNT, and Nafion on glass, with the prominent peaks marked.<sup>39,40</sup> The samples containing SWCNT were self-normalized with respect to the G peak intensity, and the Raman spectrum of the Nafion film was cross-normalized by the intensity of the G band of the Nafion/SWCNT sample. For the Nafion-coated glass sample, several peaks were observed.

These peaks have been previously attributed to  $\text{CF}_2$ , CS, COC,  $\text{SO}_3^-$ , and CC groups present in Nafion.<sup>41</sup>

For the pristine SWCNT network, peak fitting resulted in an  $I_D/I_G$  ratio of 0.021, indicating the presence of only a small number of defects.<sup>39</sup> The increase in the intensity and width of the D peak ( $1338\text{ cm}^{-1}$ ) for the Nafion/SWCNT sample is likely at least partially due to the overlap of the  $1291\text{ cm}^{-1}$  (CC degenerate stretch) and  $1372\text{ cm}^{-1}$  (CC symmetric stretch) peaks observed for Nafion. After deconvolution by the fitting of Lorentzian peaks, an  $I_D/I_G$  ratio of 0.105 was found. Similar changes have been observed previously for Nafion–CNT composites<sup>42</sup> but were attributed to damage during sonication. The  $G^-$  band peak position is shifted to higher frequencies (blue shift) when doped with electron-accepting dopants.<sup>43</sup> Blue shifts due to the doping of SWCNTs by Nafion in the range of  $2\text{--}6\text{ cm}^{-1}$  have been previously reported.<sup>44,45</sup> This p-doping was attributed to electron withdrawing of the electron-accepting electronegative  $\text{CF}_2$  groups and protonation of the SWCNTs by the acidic sulfonic groups.<sup>42,44,45</sup> This charge transfer is further evidenced by a decrease in the intensity of the  $G^-$  peak and likely also contributes to the change in the  $I_D/I_G$  ratio. Interestingly, no blue shift was observed for the  $G^+$  band, whereas the  $G^+$  was blue-shifted by  $6\text{ cm}^{-1}$  as has been observed previously for p-doping with nitric acid.<sup>13</sup>

The inset in Figure 1E shows a magnification of the radial breathing mode (RBM) peaks of the SWCNT and Nafion/SWCNT samples. The observed RBM bands for the pristine SWCNT correspond to diameters in the range of  $1.2\text{--}2.1\text{ nm}$ ,<sup>46</sup> consistent with the previous work.<sup>47</sup> One or two RBM peaks, corresponding to diameters of  $1.3$  and  $1.6\text{ nm}$ ,<sup>46</sup> were observed for the Nafion/SWCNT sample in various randomly selected spots. The appearance and intensity of RBM depend largely on the match of the laser energy, as well as the environment and SWCNT (n,m) structure.<sup>48</sup> The complete or partial disappearance of the RBM bands indicates that all or some of the doped SWCNT lost resonant enhancement. The relatively small changes after Nafion coating could be due to incomplete Nafion coverage of the SWCNTs. Nevertheless, the observed changes in the Raman spectra indicate the p-doping of the SWCNT by the Nafion coating.

**2.2. Electrochemistry.** **2.2.1. Charge Separation of Nafion/SWCNT Electrode.** Several known redox systems, including  $\text{Ru}(\text{NH}_3)_6^{2+/3+}$ ,  $\text{Fe}(\text{CN})_6^{4-/3-}$ , and  $\text{IrCl}_6^{2-/3-}$ , were used to study the electrochemical properties of the pristine SWCNT and Nafion/SWCNT electrodes. Among these, all except  $\text{Fe}(\text{CN})_6^{4-/3-}$  are generally considered to be outer-sphere redox probes, whose electron transfer is independent of surface chemistry, whereas  $\text{Fe}(\text{CN})_6^{4-/3-}$  is surface-sensitive.<sup>49</sup> The cyclic voltammograms of these measurements are shown in Figure 2, and Table S2 (Supporting Information) shows the peak potential separation ( $\Delta E_p$ ), as well as oxidation and reduction currents of the used redox probes at the bare SWCNT and the Nafion/SWCNT electrodes.

As seen from Figure 2A, both the uncoated and the Nafion-coated SWCNT electrodes show close to reversible electron transfer for  $\text{Ru}(\text{NH}_3)_6^{2+/3+}$  with  $\Delta E_p$  values of  $73.1 \pm 3.7\text{ mV}$  and  $70.7 \pm 2.2\text{ mV}$ , respectively. Furthermore, both the bare and coated electrodes show a diffusion-limited response in  $1\text{ mM Ru}(\text{NH}_3)_6^{2+/3+}$  (see Supporting Information Figure S1). A small drop in the redox current and a cathodic shift in the formal potential were also observed for  $\text{Ru}(\text{NH}_3)_6^{2+/3+}$  with the Nafion/SWCNT electrodes. Similar drops in the redox

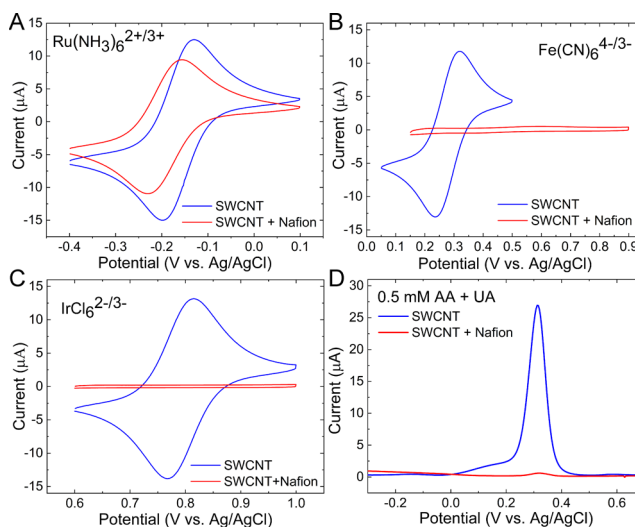


**Figure 2.** Cyclic voltammograms for SWCNT and SWCNT + Nafion electrodes in (A)  $1\text{ mM Ru}(\text{NH}_3)_6^{2+/3+}$ , (B)  $1\text{ mM Fe}(\text{CN})_6^{4-/3-}$ , and (C)  $1\text{ mM IrCl}_6^{2-/3-}$  in  $1\text{ M KCl}$ , as well as (D) differential pulse voltammogram of  $0.5\text{ mM AA}$  and  $\text{UA}$  in phosphate-buffered saline (PBS). Cyclic voltammetry (CV) scan rate of  $100\text{ mV/s}$  for all measurements.

currents and formal potential have been previously observed for Nafion-coated electrodes.<sup>50</sup>

The CVs of the negatively charged  $\text{Fe}(\text{CN})_6^{4-/3-}$  and  $\text{IrCl}_6^{2-/3-}$  are shown in Figure 2B,C, respectively. The charge exclusion of anions by the Nafion coating is evident, as the oxidation current was reduced by  $97.5\%$  for the former and totally suppressed for the latter. Moreover, the Nafion coating also caused an increase in the  $\Delta E_p$  value for  $\text{Fe}(\text{CN})_6^{4-/3-}$  from  $95.4 \pm 12.1$  to  $219.4 \pm 17.7\text{ mV}$ .

Figure 2D shows the differential pulse voltammogram of  $0.5\text{ mM}$  ascorbic acid and uric acid in PBS. It can be seen that the Nafion coating suppresses  $98.2\%$  of the AA and UA signals. Without the Nafion coating, the SWCNT electrode produces a large peak for UA that overlaps with the first oxidation peak of MO, making selective detection impossible. These results are in good agreement with the observed charge exclusion of the negatively charged redox probes (Figure 2B,C) and in line with the previous studies. Kubiak et al.<sup>24</sup> observed the permeation of  $0.6$  and  $0.7\%$  for UA and AA, respectively, in flow injection experiments with an electrode coated with recast Nafion. In the present study, however, the relative standard deviation (RSD) of the oxidation current of AA and UA was  $37\%$ . This relatively large deviation is likely caused by the large variation in the thickness of the Nafion. Similar results have also previously been explained by pinholes extending through the films.<sup>51</sup>

**2.2.2. Effect of Nafion Coating on Voltammetry of Morphine and Codeine.** Figure 3A,B shows the differential pulse voltammograms (DPVs) for morphine and codeine for both SWCNT and Nafion/SWCNT electrodes. The electrochemical oxidation of MO is known to be complex involving the oxidation of hydroxyl groups at carbons 3 and 6, as well as the electrochemical demethylation of the aliphatic tertiary amine. The oxidation peak for morphine, which is most frequently used for determining MO,<sup>23,28,31,33,52</sup> occurs at around  $+0.4\text{ V}$  and has been previously attributed to the oxidation of the phenolic group.<sup>28</sup> This is followed by chemical reactions leading to dimerization and formation of pseudo-

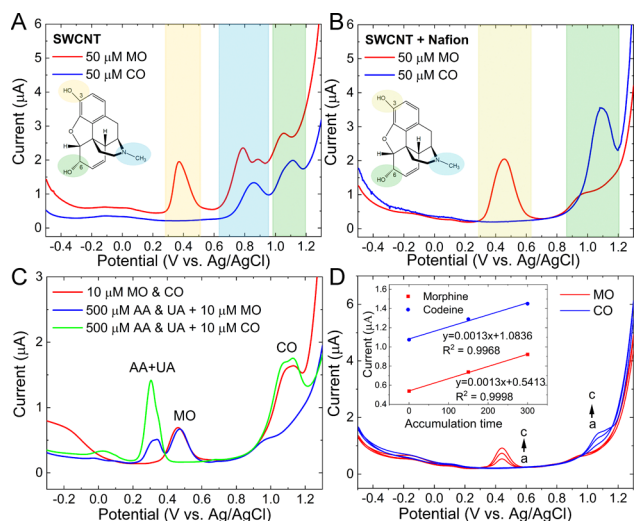


**Figure 3.** Simultaneous detection of MO and CO in PBS. Differential pulse voltammograms for (A) SWCNT and (B) SWCNT + Nafion electrodes and assignment of the oxidation peaks in 50  $\mu\text{M}$  MO and CO, (C) individual and simultaneous detection of 10  $\mu\text{M}$  MO and CO in the presence and absence of 500  $\mu\text{M}$  AA and UA with SWCNT + Nafion electrodes, and (D) 10  $\mu\text{M}$  MO and CO with accumulation times of (a) 0 s, (b) 150 s, and (c) 300 s.

morphine. The peak occurring at around +0.8 V for MO has been attributed to the oxidation of the aliphatic tertiary amine. The shoulder observed for this peak at +0.85 V can be explained by further oxidation of the secondary aliphatic amine that forms due to reaction with water in aqueous electrolytes.<sup>28</sup> Interestingly, this second peak is not as well defined for codeine. The last observed peak has been previously attributed to the hydroxyl group at the 6-carbon.

For codeine, two peaks close to each other are observed related to the oxidation of the tertiary amine and the 6-hydroxyl group. Codeine lacks the peak at around +0.4 V as the hydroxyl group at the 3-carbon is substituted for a methoxy group. For the SWCNT electrode, it is evident that the MO oxidation peaks for the hydroxyl group at the 6-carbon and that of the amine overlap with those of codeine, possessing the same amine and 6-carbon hydroxyl functionalities. As can be seen from Figure 3B,C, the oxidation peaks likely attributed to the amine are not observed with the Nafion/SWCNT electrode. It should be noted, however, that there is a very large variation in the voltammetric responses of MO and CO in the literature,<sup>10,27,28,33,37,53</sup> making reliable assignment of the peaks challenging. Moreover, voltammetric response with only one peak for MO and CO has been previously observed with some metal-oxide-based electrodes.<sup>10,37</sup> Likewise, Ensafi et al.<sup>53</sup> reported similar voltammetric responses for MO and CO in the ionic liquid *N*-hexyl-3-methylimidazolium hexafluorophosphate. They also attributed the observed peaks to the oxidation of hydroxyl groups at carbons 3 and 6 for MO and CO, respectively. We have also recently observed similar behavior for tramadol and *O*-desmethyltramadol at a tetrahedral amorphous carbon electrode coated with Nafion.<sup>9</sup> It is well known that electron-withdrawing substituents increase the oxidation potential of aliphatic tertiary amines.<sup>54</sup> Interactions with the Teflon or the sulfonic groups of the Nafion could cause the observed changes in the voltammetry of MO and CO. Similar changes to the oxidation potential of the hydroxyl group at the 6-carbon can, however, not be ruled

out without further research. The Nafion/SWCNT electrode, however, produces a well-defined peak at +0.44 V related to the oxidation of the phenolic group of morphine.<sup>28</sup> This represents an 80 mV anodic shift from the uncoated electrode and results in better peak separation between the residual peak for UA and the MO peak. A second poorly defined broad peak centered at +0.98 V was also observed, likely due to the oxidation of the hydroxyl group at carbon 6. Likewise, only one primary peak was observed for CO at the Nafion/SWCNT electrode. At lower concentrations, however, two partially overlapping peaks can be observed for CO at the Nafion/SWCNT electrode, indicating the existence of two overlapping peaks. It is currently unclear what causes these changes in the voltammetry of MO and CO and what role the Nafion coating and its potential p-doping has on the voltammetry of these opioids. Further work is required to understand why morphine and codeine behave as they do at Nafion electrodes. To verify the charge selectivity, DPV measurements were carried out in the absence and presence of 500  $\mu\text{M}$  AA and UA. Figure 3C shows that despite the large variation in the oxidation current of AA and UA, the oxidation currents of MO and CO changed only by 3.0 and 6.5%, which are within the electrode-to-electrode variation of this work. Figure 3C further shows that similar currents are obtained for MO and CO in the presence and absence of 10  $\mu\text{M}$  of the other opioid, indicating that the simultaneous detection of MO and CO is possible without interference.

Although exchange equilibrium between Nafion and water is rapid for small cations, larger ions exchange more slowly, and owing to this kinetic effect, they require longer equilibrium times. Figure 3A,B shows an increase in the signal of MO and CO with the Nafion/SWCNT electrode compared to that of the bare SWCNT electrodes with an accumulation time of 300 s, likely due to the preconcentration of morphine and codeine. For this reason, the effect of the accumulation time was studied. The results shown in Figure 3D indicate the accumulation of 10  $\mu\text{M}$  MO and CO under open-circuit conditions. A linear increase in current with increasing accumulation time was found. The slopes for MO and CO were almost identical, indicating similar enrichment behavior. Note that similar behavior was not observed for the uncoated electrodes. The accumulation time was limited to 300 s for practical reasons and to achieve a measurement protocol that is rapid in nature.

**2.2.3. Simultaneous Determination of Morphine and Codeine.** Several concentrations of MO in the presence of 10  $\mu\text{M}$  CO and vice versa were measured. Both DPV measurements shown in Figure 4A,C were carried out in the presence of 0.5 mM ascorbic acid and uric acid. The electrode utilized in this work can be seen to measure currents above the baseline for 50 nM MO and 100 nM CO. For MO, there were two linear relations with different slopes. In the low-concentration range (0.05–1  $\mu\text{M}$ ), a linear regression equation of  $I_{\text{pa}}(\mu\text{A}) = 0.0859C_{\text{MO}} + 0.1430$  ( $R^2 = 0.9992$ ) was obtained. In the higher-concentration range (1–10  $\mu\text{M}$ ), the electrodes showed a second linear regression equation of  $I_{\text{pa}}(\mu\text{A}) = 0.0500C_{\text{MO}} + 0.1994$  ( $R^2 = 0.9885$ ). Other works have also reported two linear ranges for morphine.<sup>31,52</sup> It could be that higher concentrations cause saturation of the available surface sites for the electrochemical oxidation of morphine. It is also possible that prolonged measurements with many concentrations cause some fouling and passivation of the electrode. After 10  $\mu\text{M}$ , the slope deviated from the linear relationship,

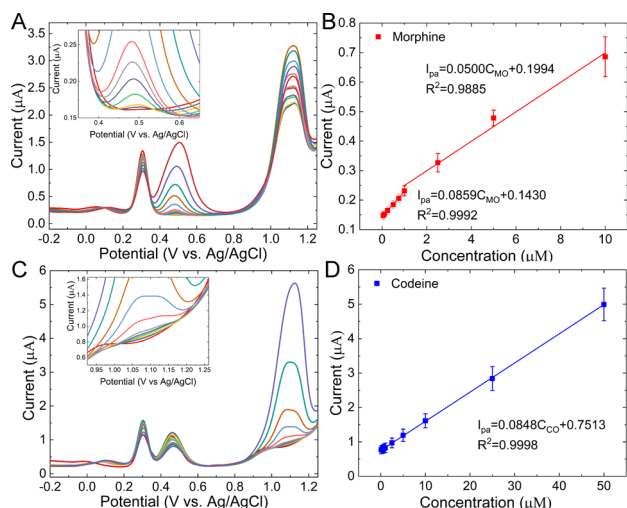


**Figure 4.** Linear ranges of MO and CO in PBS. Differential pulse voltammograms of (A) 10  $\mu\text{M}$  CO and 0, 0.05, 0.1, 0.25, 0.5, 0.75, 1, 2.5, 5, 10, 25, and 50  $\mu\text{M}$  MO, and (C) 10  $\mu\text{M}$  MO and 0, 0.1, 0.25, 0.5, 0.75, 1, 2.5, 5, 10, 25, and 50  $\mu\text{M}$  CO. Both (A) and (C) are in the presence of 0.5 mM AA and UA. The average currents with standard deviations ( $n = 3$ ) with linear fits for (B) MO and (D) CO.

likely due to the passivation of the electrode surface. For codeine, only one linear range  $I_{pa}(\mu\text{A}) = 0.0848C_{CO} + 0.7513$  ( $R^2 = 0.9998$ ) was found (0.1–50  $\mu\text{M}$ ). The relatively narrow linear ranges seem to be typical of many electrode materials for morphine.<sup>31,33</sup>

Based on the sensitivities and the standard deviation of the current in three consecutive measurements in blank solutions, limits of detection (LOD) were calculated. LODs of 0.071 and

0.277  $\mu\text{M}$  for MO and CO, respectively, were obtained. These detection limits represent clinically relevant concentrations of MO and CO.

As shown in Table 1, lower detection limits have been achieved for individual detection of MO and CO in the presence of AA and UA. Švorc et al.<sup>35</sup> reported the selective detection of CO alone in the presence of AA and UA. Similarly, the selective detection of MO in the presence of AA and UA has been reported with the use of surfactants<sup>31</sup> and medium exchange.<sup>29</sup> Atta et al.<sup>23</sup> also reported increased selectivity at a Nafion-based electrode in large excess of UA. However, the concentration difference between MO and AA and UA was considerably smaller than in the present work. Moreover, there is no evidence that these electrodes would be capable of simultaneous detection of MO and CO.

Lower detection limits have also been observed for the simultaneous detection of MO and CO at various metal-based electrode platforms (Table 1). These studies, however, did not investigate the interference of AA and UA or reported interference in large excess of AA and UA.<sup>37</sup> As a result, these electrodes have to rely on considerable dilution and spiking of real samples to avoid matrix effects. Simultaneous detection of MO and CO has also been reported in 1000-fold excess of AA and UA, individually. The reported detection mechanism is, however, based on a more complicated DNA functionalized biosensor with electrochemical detection.<sup>38</sup>

While the current of the UA and AA peaks showed a considerable relative standard deviation (RSD) of 37% from electrode to electrode ( $n = 6$ ), satisfactory RSD values of 7.3 and 13.9% ( $n = 3$ ) for MO and CO, respectively, were achieved. These relatively large variations are likely due to the variation in the thickness of the Nafion coating or pinholes extending through the film. The performance of the electrode

**Table 1. Comparison of Electrochemical Detection of MO and CO with Various Electrode Platforms Along with the Used Method, Limits of Detection (LOD), Linear Ranges, and Interference of AA and UA**

electrode	method	MO LOD ( $\mu\text{M}$ )	linear range MO ( $\mu\text{M}$ )	CO LOD ( $\mu\text{M}$ )	linear range CO ( $\mu\text{M}$ )	interference of AA and UA (tolerance)	ref
Au NP/Nafion CPE	DPV	0.00133	0.2–260			AA (5 mM) UA (5 mM)	23
AP Ti/ta-C	DPV	0.0098	0.1–10				33
PEDOT/Pt	DPV	0.05	0.3–8			AA (50 mM) UA (5 mM)	31
		0.06	10–60				
OMC/GCE	CV	0.05	0.1–20				29
EC pretreated GC	CV	0.2	4–18				52
			18–100				
GR-Nafion/GCE	SWV			0.015	0.05–9	AA (<0.012 mM) UA (<0.15 mM)	34
BDD	DPV			0.08	0.1–60	UA (2 mM) AA (2 mM)	35
dsDNA/MWCNT-PDDA/PGE	DPV	0.14	0.16–140	0.13	0.16–140	AA (5.68 mM) UA (5.95 mM)	38
PB/Pd-Al	Amp.	0.8	2–50	0.8	2–30		36
Zn <sub>2</sub> SnO <sub>4</sub> -GO/CPE	DPV	0.011	0.020–15	0.009	0.020–15	AA (0.2 mM)	10
MWCNTs/SnO <sub>2</sub> -Zn <sub>2</sub> SnO <sub>4</sub> /CPE	DPV	0.009	0.1–310	0.009	0.1–600	AA <sup>a</sup> UA <sup>a</sup>	37
Nafion/SWCNT	DPV	0.071	0.05–1	0.277	0.1–50	AA (0.5 mM)	this work
			1–10			UA (0.5 mM)	

<sup>a</sup>Caused interference with MO and CO.

can likely be improved by further development of the Nafion deposition process.

#### 2.2.4. Measurement of Morphine and Codeine in Plasma.

To verify the applicability of the developed electrode in real samples, DPV measurements were carried out in human plasma, diluted two times with PBS. Figure 5A shows the blank

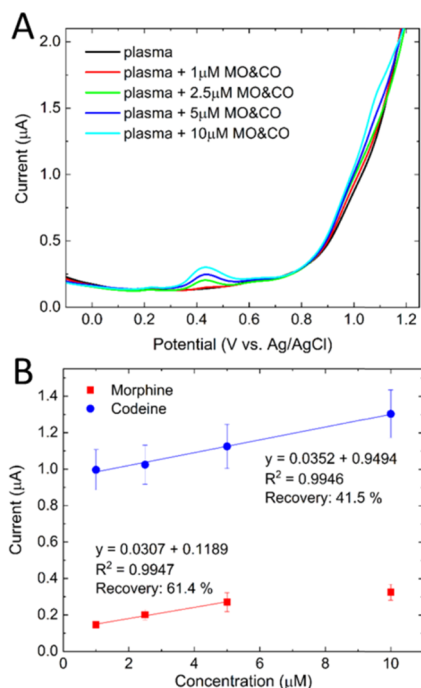


**Figure 5.** Differential pulse voltammetry measurements in human plasma. (A) DPV of increasing concentrations of MO and CO in plasma and (B) linear ranges of the measurements with standard deviations as error bars ( $n = 5$ ). Accumulation time 5 min.

scan in plasma and after spiking with increasing amounts of MO and CO. The oxidation currents scaled linearly with the concentration in the range of 1–5  $\mu\text{M}$  for MO and 1–10  $\mu\text{M}$  for CO. The background currents in blank plasma show virtually no matrix effect for MO, whereas the background current is slightly increased for CO. It should be noted that no precipitation of proteins was carried out before measurements. All comparable studies in Table 1 precipitated the proteins and diluted their samples at least 5-fold. Moreover, none of the studies have assessed the effects of drug plasma protein binding on the detection capabilities of the electrodes. In this work, recoveries based on the sensitivities in the linear range were 61.4 and 41.5% for MO and CO, respectively. The RSD values for MO and CO were 13 and 10%, respectively, comparable to those measured in large excess of AA and UA.

Unbound fractions of 53–68% for MO and 44% for CO have been reported in previous studies.<sup>55–57</sup> Despite large variations between the few available studies, the comparison of the unbound fractions with the recovery percentages in our study (61.4% for MO and 41.5% for CO) suggests that the electrode may, in fact, be measuring the clinically interesting free fraction of MO and CO in plasma.

To verify that the lower recoveries are not due to rapid passivation of the electrode or blocking of the ionic channels of the Nafion film, two electrodes were measured for three consecutive times in plasma with 10  $\mu\text{M}$  MO and CO. The RSDs for these measurements were 2.7 and 4.2% for MO and

CO, respectively, indicating no further passivation of the electrode. A further passivation study with  $\text{Ru}(\text{NH}_3)_6^{2+/3+}$  in PBS and the diluted human plasma was also carried out. No meaningful difference was observed in the redox currents in the CV measurements of 1 mM  $\text{Ru}(\text{NH}_3)_6^{2+/3+}$  in PBS and diluted human plasma shown in Figure S2 in the Supporting Information. While there may be adsorption of proteins on the surface of the electrode, there seems to be no apparent blocking of the ionic channels of the Nafion coating. It should be noted that these results do not completely rule out the possibility of fouling of the active sites of inner-sphere analytes, such as MO and CO, as a cause for the reduced recoveries. More studies with a wider range of analytes with and without protein precipitation combined with equilibrium dialysis are required to fully understand these plasma measurements.

Nonetheless, these measurements show that it is possible to measure close to therapeutic concentrations of MO and CO without considerable dilution of the plasma or precipitation of the proteins. Despite these interesting results, the large electrode-to-electrode variation in the CO oxidation current makes the measurement of CO with concentrations below 2.5  $\mu\text{M}$  challenging. This is likely due to both the lower sensitivity toward CO and the low recovery, presumably due to the high protein-bound fraction of CO. These challenges could, however, be at least partially overcome with further optimization of the multilayer electrode and by spiking of the supporting electrolyte, as is commonly done in many analysis methods.

### 3. CONCLUSIONS

In this work, we fabricated disposable dual-layer SWCNT/Nafion electrodes. We showed that SWCNT network electrodes could be easily fabricated through a simple dry transfer method and coated with Nafion through dip-coating. The Nafion coating was shown to alter the voltammetry of MO and CO, enabling their simultaneous detection. In addition, the fabricated electrode showed charge exclusion of anions and enrichment of MO and CO. These properties make nanomolar detection of MO and CO possible in large excess of AA and UA. Simultaneous detection of MO and CO close to physiologically relevant concentrations was also achieved in the presence of AA and UA, as well as in human plasma with only mild dilution without the precipitation of proteins. Recoveries closely matching those previously reported for unbound fractions of MO and CO were obtained in human plasma.

### 4. EXPERIMENTAL SECTION

#### 4.1. Single-Walled Carbon Nanotube Synthesis.

SWCNTs were synthesized by thermal high-temperature floating catalyst chemical vapor deposition. The process is described in greater detail in refs 13 and 58. In this process, iron nanoparticles are formed through thermal decomposition of ferrocene in a carbon monoxide atmosphere. The iron nanoparticles catalyze the decomposition of carbon monoxide, leading to nucleation and growth of SWCNT in the gas phase inside a quartz laminar flow reactor. The formed SWCNTs form bundles in gas phase<sup>59</sup> and are collected on nitrocellulose membranes.

**4.2. Electrode Fabrication.** The SWCNT networks were press-transferred onto glass (Thermo Scientific, ISO 8037-1) and densified. The room-temperature press-transfer process is

described in detail in refs 13 and 14. Briefly, the glass was precleaved to  $1 \times 2 \text{ cm}^2$  pieces and cleaned by sonication in acetone (AnalaR NORMAPUR, Merck). After cleaning, the pieces were blown by nitrogen. The filters with the SWCNT networks were cut and placed on the glass pieces with the SWCNT side down and pressed between two glass slides. After carefully peeling off the filter backing, the adhered SWCNT network was densified with a few drops of ethanol as in ref 13 and baked at  $70 \text{ }^\circ\text{C}$  for 3 min.

Silver contact pads were prepared with conductive silver paint (Electrolube). The silver was dried at room temperature for 15 min and baked on a hot plate preheated to  $60 \text{ }^\circ\text{C}$  for 3 min. The electrode was then covered with a PTFE film (Saint-Gobain Performance Plastics CHR 2255-2) with a 3 mm hole. Finally, the electrode was dip-coated by immersing the electrode for 5 s in 5 wt % Nafion 117 solution (Sigma-Aldrich). Before measurements, the electrode was allowed to dry under ambient conditions overnight. A scheme of the step-by-step electrode fabrication is shown in Figure S3 in the Supporting Information.

**4.3. Characterization.** The SWCNT networks grown under the same conditions have been characterized in previous work by scanning electron microscopy (SEM), atomic force microscopy (AFM), transmission electron microscopy (TEM), and X-ray photoelectron spectroscopy (XPS).<sup>14,47</sup> Based on TEM and AFM analyses, bundle sizes of 3–20 nm were found. The XPS survey spectrum of the SWCNT networks press-transferred onto oxidized Si wafer showed peaks for silicon, oxygen, and carbon. More detailed TEM investigations were performed in the present study by an FEI Tecnai F-20 TEM at a 200 kV acceleration voltage. Specimens were prepared by press-transferring the SWCNT network directly onto M75 copper-only TEM grids (Agar). Energy-dispersive spectroscopy (EDS) was also performed in scanning transmission electron microscopy (STEM) mode on multiple  $6.5 \times 6.5 \text{ }\mu\text{m}^2$  areas ( $n = 7$ ).

Cross-sectional scanning electron microscopy (SEM) samples were prepared by cleaving Nafion/SWCNT electrodes. Prior to cleaving, the electrodes were cooled in liquid nitrogen. Before imaging, the cross section was coated with 2 nm Au by sputtering (Leica EM SCD050). The thickness of the Nafion membrane was measured from the cross-sectional SEM images obtained with an S-4700 SEM (Hitachi). Visible Raman spectroscopy was performed with a LabRAM HR (Jobin Yvon Horiba) confocal Raman system. An argon laser with  $\lambda = 514 \text{ nm}$  (power 10 mW) and BX41 (Olympus) microscope with a 100 $\times$  objective (spot size of less than  $1 \text{ }\mu\text{m}$ ) was used.

**4.4. Electrochemistry.** Cyclic voltammetry (CV) and differential pulse voltammetry (DPV) measurements were carried out with a CH Instrument (CHI630E) potentiostat. A three-electrode cell was used for all electrochemical measurements with a Ag/AgCl electrode as reference ( $+0.199 \text{ V}$  vs SHE, Radiometer Analytical) and a Pt wire as the counter electrode. All chemicals were obtained from Sigma-Aldrich, unless stated otherwise. Morphine hydrochloride and codeine hydrochloride were obtained from the University Pharmacy, Helsinki, Finland.

The electrochemical properties of SWCNT and Nafion/SWCNT electrodes were studied with hexammineruthenium(III)chloride, potassium hexacyanoferrate(III), and potassium hexachloroiridate(IV) redox probes. Solutions with concentrations of 1 mM of each probe were prepared in 1 M KCl

(Merck Suprapur). Both electrode types were measured with each redox probe with several scan rates at room temperature. Solutions of 500  $\mu\text{M}$  L-ascorbic acid and 500  $\mu\text{M}$  uric acid were prepared in phosphate-buffered saline (PBS) solution with pH 7.4. Stock solutions of 1 mM of MO and CO were also prepared in PBS and injected into the cell to achieve increasing concentrations. All DPV measurements were conducted with a pulse amplitude of 50 mV and a scan rate of 20 mV/s. The electrodes were placed in blank PBS solutions between measurements. Prior to all, except for the plasma measurements, the solutions were deoxygenated with nitrogen for at least 5 min, and the cell was blanketed throughout the measurements.

For the plasma measurements, expired human plasma (Octaplas AB, Sweden) was received from the blood center of HUSLAB (Finland). Plasma (5 mL) was diluted with 5 mL of PBS and measured without further processing. Equal additions of MO and CO stock solutions were injected into the cell to achieve concentrations of 1, 2.5, 5, and 10  $\mu\text{M}$ . DPVs were measured with an accumulation time of 5 min and a 5 min washout in PBS between each concentration. Hexammineruthenium(III)chloride (1 mM) was also measured with CV in both diluted plasma and PBS to study the passivation of the electrode.

## ■ ASSOCIATED CONTENT

### Supporting Information

The Supporting Information is available free of charge on the ACS Publications website at DOI: 10.1021/acsomega.9b02147.

STEM EDS analysis results from seven randomly selected  $6.5 \times 6.5 \text{ }\mu\text{m}^2$  areas; peak potential separations  $\Delta E_p$ , oxidation and reduction currents for  $\text{Ru}(\text{NH}_3)_6^{2+/3+}$ ,  $\text{Fe}(\text{CN})_6^{4-/3-}$ , and  $\text{IrCl}_6^{2-/3-}$  at bare SWCNT and Nafion/SWCNT electrodes; cyclic voltammetry oxidation ( $I_{pa}$ ) and reduction ( $I_{pc}$ ) currents as a function of the square root of the scan rate in 1 mM  $\text{Ru}(\text{NH}_3)_6^{2+/3+}$  in 1 M KCl; cyclic voltammogram of the Nafion-coated SWCNT electrode in 1 mM  $\text{Ru}(\text{NH}_3)_6^{2+/3+}$  in pH 7.4 PBS and in a 1:2 diluted human plasma without the precipitation of proteins (PDF)

## ■ AUTHOR INFORMATION

### Corresponding Author

\*E-mail: niklas.wester@aalto.fi.

### ORCID

Niklas Wester: 0000-0002-7937-9011

Jarkko Etula: 0000-0002-6930-1165

Tomi Laurila: 0000-0002-1252-8764

### Notes

The authors declare no competing financial interest.

## ■ ACKNOWLEDGMENTS

This work was supported by Business Finland (FEDOC project, grant number 211637 and FEPOD-TUTLI project, grant number 211773). Dr. Jenni Viinamäki, Department of Clinical Pharmacology, University of Helsinki, is acknowledged for expert assistance and providing plasma samples. The authors also acknowledge the provisions of facilities of Otanano.

## REFERENCES

- (1) Wiffen, P. J.; Wee, B.; Derry, S.; Bell, R. F.; Moore, R. A. Opioids for Cancer Pain - an Overview of Cochrane Reviews *Cochrane Database Syst. Rev.* 2017, 7, 012592. DOI: 10.1002/14651858.CD012592.pub2.
- (2) Schug, S. A.; Sidebotham, D. A.; McGuinness, M.; Thomas, J.; Fox, L. Acetaminophen as an Adjunct to Morphine by Patient-Controlled Analgesia in the Management of Acute Postoperative Pain. *Anesth. Analg.* 1998, 87, 368–372.
- (3) Kirchheiner, J.; Schmidt, H.; Tzvetkov, M.; Keulen, J.-T.; Lötsch, J.; Roots, I.; Brockmüller, J. Pharmacokinetics of Codeine and Its Metabolite Morphine in Ultra-Rapid Metabolizers Due to CYP2D6 Duplication. *Pharmacogenomics J.* 2007, 7, 257–265.
- (4) Gasche, Y.; Daali, Y.; Fathi, M.; Chiappe, A.; Cottini, S.; Dayer, P.; Desmeules, J. Codeine Intoxication Associated with Ultrarapid CYP2D6 Metabolism. *N. Engl. J. Med.* 2004, 351, 2827–2831.
- (5) Voronov, P.; Przybylo, H. J.; Jagannathan, N. Apnea in a Child after Oral Codeine: A Genetic Variant? An Ultra-Rapid Metabolizer. *Pediatr. Anesth.* 2007, 17, 684–687.
- (6) Kelly, L. E.; Rieder, M.; van den Anker, J.; Malkin, B.; Ross, C.; Neely, M. N.; Carleton, B.; Hayden, M. R.; Madadi, P.; Koren, G. More Codeine Fatalities After Tonsillectomy in North American Children. *Pediatrics* 2012, 129, e1343–e1347.
- (7) Hoskin, P.; Hanks, G.; Aherne, G.; Chapman, D.; Littleton, P.; Filshie, J. The Bioavailability and Pharmacokinetics of Morphine after Intravenous, Oral and Buccal Administration in Healthy Volunteers. *Br. J. Clin. Pharmacol.* 1989, 27, 499–505.
- (8) Konstantinova, S. V.; Normann, P. T.; Arnestad, M.; Karinen, R.; Christophersen, A. S.; Mørland, J. Morphine to Codeine Concentration Ratio in Blood and Urine as a Marker of Illicit Heroin Use in Forensic Autopsy Samples. *Forensic Sci. Int.* 2012, 217, 216–221.
- (9) Mynttinen, E.; Wester, N.; Lilius, T.; Kalso, E.; Koskinen, J.; Laurila, T. Simultaneous Electrochemical Detection of Tramadol and O-Desmethyltramadol with Nafion-Coated Tetrahedral Amorphous Carbon Electrode. *Electrochim. Acta* 2019, 295, 347–353.
- (10) Bagheri, H.; Khoshshafar, H.; Afkhami, A.; Amidi, S. Sensitive and Simple Simultaneous Determination of Morphine and Codeine Using a Zn<sub>2</sub> SnO<sub>4</sub> Nanoparticle/Graphene Composite Modified Electrochemical Sensor. *New J. Chem.* 2016, 40, 7102–7112.
- (11) Afkhami, A.; Khoshshafar, H.; Bagheri, H.; Madrakian, T. Facile Simultaneous Electrochemical Determination of Codeine and Acetaminophen in Pharmaceutical Samples and Biological Fluids by Graphene-CoFe<sub>2</sub>O<sub>4</sub> Nanocomposite Modified Carbon Paste Electrode. *Sens. Actuators, B* 2014, 203, 909–918.
- (12) Laurila, T.; Sainio, S.; Caro, M. A. Hybrid Carbon Based Nanomaterials for Electrochemical Detection of Biomolecules. *Prog. Mater. Sci.* 2017, 88, 499–594.
- (13) Kaskela, A.; Nasibulin, A. G.; Timmermans, M. Y.; Aitchison, B.; Papadimitratos, A.; Tian, Y.; Zhu, Z.; Jiang, H.; Brown, D. P.; Zakhidov, A.; et al. Aerosol-Synthesized SWCNT Networks with Tunable Conductivity and Transparency by a Dry Transfer Technique. *Nano Lett.* 2010, 10, 4349–4355.
- (14) Iyer, A.; Kaskela, A.; Johansson, L.-S.; Liu, X.; Kauppinen, E. I.; Koskinen, J. Single Walled Carbon Nanotube Network—Tetrahedral Amorphous Carbon Composite Film. *J. Appl. Phys.* 2015, 117, No. 225302.
- (15) Sun, D.; Timmermans, M. Y.; Tian, Y.; Nasibulin, A. G.; Kauppinen, E. I.; Kishimoto, S.; Mizutani, T.; Ohno, Y. Flexible High-Performance Carbon Nanotube Integrated Circuits. *Nat. Nanotechnol.* 2011, 6, 156–161.
- (16) Ames, B. N.; Cathcart, R.; Schwiers, E.; Hochstein, P. Uric Acid Provides an Antioxidant Defense in Humans against Oxidant- and Radical-Caused Aging and Cancer: A Hypothesis. *Proc. Natl. Acad. Sci. U.S.A.* 1981, 78, 6858–6862.
- (17) Heiskanen, T.; Langel, K.; Gunnar, T.; Lillsunde, P.; Kalso, E. A. Opioid Concentrations in Oral Fluid and Plasma in Cancer Patients With Pain. *J. Pain Symptom Manage.* 2015, 50, 524–532.
- (18) Osborne, R.; Joel, S.; Trew, D.; Slevin, M. Morphine and Metabolite Behavior after Different Routes of Morphine Administration: Demonstration of the Importance of the Active Metabolite Morphine-6-Glucuronide. *Clin. Pharmacol. Ther.* 1990, 47, 12–19.
- (19) Goucke, R. C.; Hackett, P. L.; Ilett, K. F. Concentrations of Morphine, Morphine-6-Glucuronide and Morphine-3-Glucuronide in Serum and Cerebrospinal Fluid Following Morphine Administration to Patients with Morphine-Resistant Pain. *Pain* 1994, 56, 145–149.
- (20) Drummer, O. H. Postmortem Toxicology of Drugs of Abuse. *Forensic Sci. Int.* 2004, 142, 101–113.
- (21) Quiding, H.; Anderson, P.; Bondesson, U.; Boréus, L. O.; Hynning, P. Plasma Concentrations of Codeine and Its Metabolite, Morphine, after Single and Repeated Oral Administration. *Eur. J. Clin. Pharmacol.* 1986, 30, 673–677.
- (22) Chen, C.-H.; Luo, S.-C. Tuning Surface Charge and Morphology for the Efficient Detection of Dopamine under the Interferences of Uric Acid, Ascorbic Acid, and Protein Adsorption. *ACS Appl. Mater. Interfaces* 2015, 7, 21931–21938.
- (23) Atta, N. F.; Galal, A.; Azab, S. M. Determination of Morphine at Gold Nanoparticles/Nafion Carbon Paste Modified Sensor Electrode. *Analyst* 2011, 136, 4682–4691.
- (24) Kubiak, W. W.; Wang, J. Flow Injection Analysis as a Tool for Studying Polymer Modified Electrodes. *Anal. Chim. Acta* 1996, 329, 181–189.
- (25) Rocha, L. S.; Carapuça, H. M. Ion-Exchange Voltammetry of Dopamine at Nafion-Coated Glassy Carbon Electrodes: Quantitative Features of Ion-Exchange Partition and Reassessment on the Oxidation Mechanism of Dopamine in the Presence of Excess Ascorbic Acid. *Bioelectrochemistry* 2006, 69, 258–266.
- (26) Trouillon, R.; Combs, Z.; Patel, B. A.; O'Hare, D. Comparative Study of the Effect of Various Electrode Membranes on Biofouling and Electrochemical Measurements. *Electrochem. Commun.* 2009, 11, 1409–1413.
- (27) Garrido, J. M. P. J.; Delerue-Matos, C.; Borges, F.; Macedo, T. R. A.; Oliveira-Brett, A. M. Voltammetric Oxidation of Drugs of Abuse II. Codeine and Metabolites. *Electroanalysis* 2004, 16, 1427–1433.
- (28) Garrido, J. M. P. J.; Delerue-Matos, C.; Borges, F.; Macedo, T. R. A.; Oliveira-Brett, A. M. Voltammetric Oxidation of Drugs of Abuse I. Morphine and Metabolites. *Electroanalysis* 2004, 16, 1419–1426.
- (29) Li, F.; Song, J.; Shan, C.; Gao, D.; Xu, X.; Niu, L. Electrochemical Determination of Morphine at Ordered Mesoporous Carbon Modified Glassy Carbon Electrode. *Biosens. Bioelectron.* 2010, 25, 1408–1413.
- (30) Nigović, B.; Sadiković, M.; Sertić, M. Multi-Walled Carbon Nanotubes/Nafion Composite Film Modified Electrode as a Sensor for Simultaneous Determination of Ondansetron and Morphine. *Talanta* 2014, 122, 187–194.
- (31) Atta, N. F.; Galal, A.; Ahmed, R. A. Direct and Simple Electrochemical Determination of Morphine at PEDOT Modified Pt Electrode. *Electroanalysis* 2011, 23, 737–746.
- (32) Dehdashtian, S.; Gholivand, M. B.; Shamsipur, M.; Kariminia, S. Construction of a Sensitive and Selective Sensor for Morphine Using Chitosan Coated Fe<sub>3</sub>O<sub>4</sub> Magnetic Nanoparticle as a Modifier. *Mater. Sci. Eng., C* 2016, 58, 53–59.
- (33) Wester, N.; Etula, J.; Lilius, T.; Sainio, S.; Laurila, T.; Koskinen, J. Selective Detection of Morphine in the Presence of Paracetamol with Anodically Pretreated Dual Layer Ti/Tetrahedral Amorphous Carbon Electrodes. *Electrochem. Commun.* 2018, 86, 166–170.
- (34) Li, Y.; Li, K.; Song, G.; Liu, J.; Zhang, K.; Ye, B. Electrochemical Behavior of Codeine and Its Sensitive Determination on Graphene-Based Modified Electrode. *Sens. Actuators, B* 2013, 182, 401–407.
- (35) Švorc, L.; Sochr, J.; Švitková, J.; Rievaj, M.; Dušan, B. Rapid and Sensitive Electrochemical Determination of Codeine in Pharmaceutical Formulations and Human Urine Using a Boron-Doped Diamond Film Electrode. *Electrochim. Acta* 2013, 87, 503–510.
- (36) Pournaghi-Azar, M. H.; Saadatirad, A. Simultaneous Voltammetric and Amperometric Determination of Morphine and Codeine

Using a Chemically Modified-Palladized Aluminum Electrode. *J. Electroanal. Chem.* **2008**, *624*, 293–298.

(37) Taei, M.; Hasanpour, F.; Hajhashemi, V.; Movahedi, M.; Baghlani, H. Simultaneous Detection of Morphine and Codeine in Urine Samples of Heroin Addicts Using Multi-Walled Carbon Nanotubes Modified SnO<sub>2</sub>-Zn<sub>2</sub>SnO<sub>4</sub> Nanocomposites Paste Electrode. *Appl. Surf. Sci.* **2016**, *363*, 490–498.

(38) Ensafi, A. A.; Heydari-Bafrooei, E.; Rezaei, B. Different Interaction of Codeine and Morphine with DNA: A Concept for Simultaneous Determination. *Biosens. Bioelectron.* **2013**, *41*, 627–633.

(39) Jorio, A.; Saito, R.; Dresselhaus, G.; Dresselhaus, M. S. Determination of Nanotubes Properties by Raman Spectroscopy. *Philos. Trans. R. Soc., A* **2004**, *362*, 2311–2336.

(40) Fantini, C.; Pimenta, M. A.; Strano, M. S. Two-Phonon Combination Raman Modes in Covalently Functionalized Single-Wall Carbon Nanotubes. *J. Phys. Chem. C* **2008**, *112*, 13150–13155.

(41) Bribes, J.-L.; El Boukari, M.; Maillols, J. Application of Raman Spectroscopy to Industrial Membranes. Part 2—Perfluorosulphonic Membrane. *J. Raman Spectrosc.* **1991**, *22*, 275–279.

(42) Zhang, J.; Gao, L.; Sun, J.; Liu, Y.; Wang, Y.; Wang, J.; Kajiura, H.; Li, Y.; Noda, K. Dispersion of Single-Walled Carbon Nanotubes by Nafion in Water/Ethanol for Preparing Transparent Conducting Films. *J. Phys. Chem. C* **2008**, *112*, 16370–16376.

(43) Rao, A. M.; Eklund, P. C.; Bandow, S.; Thess, A.; Smalley, R. E. Evidence for Charge Transfer in Doped Carbon Nanotube Bundles from Raman Scattering. *Nature* **1997**, *388*, 257–259.

(44) Geng, H.-Z.; Kim, K. K.; Song, C.; Xuyen, N. T.; Kim, S. M.; Park, K. A.; Lee, D. S.; An, K. H.; Lee, Y. S.; Chang, Y.; et al. Doping and De-Doping of Carbon Nanotube Transparent Conducting Films by Dispersant and Chemical Treatment. *J. Mater. Chem.* **2008**, *18*, 1261.

(45) Engtrakul, C.; Davis, M. F.; Gennett, T.; Dillon, A. C.; Jones, K. M.; Heben, M. J. Protonation of Carbon Single-Walled Nanotubes Studied Using <sup>13</sup>C and <sup>1</sup>H-<sup>13</sup>C Cross Polarization Nuclear Magnetic Resonance and Raman Spectroscopies. *J. Am. Chem. Soc.* **2005**, *127*, 17548–17555.

(46) Dresselhaus, M. S.; Dresselhaus, G.; Saito, R.; Jorio, A. Raman Spectroscopy of Carbon Nanotubes. *Phys. Rep.* **2005**, *409*, 47–99.

(47) Iyer, A.; Kaskela, A.; Novikov, S.; Etula, J.; Liu, X.; Kauppinen, E. I.; Koskinen, J. Effect of Tetrahedral Amorphous Carbon Coating on the Resistivity and Wear of Single-Walled Carbon Nanotube Network. *J. Appl. Phys.* **2016**, *119*, No. 185306.

(48) Tian, Y.; Jiang, H.; Laiho, P.; Kauppinen, E. I. Validity of Measuring Metallic and Semiconducting Single-Walled Carbon Nanotube Fractions by Quantitative Raman Spectroscopy. *Anal. Chem.* **2018**, *90*, 2517–2525.

(49) Mccreery, R. L. Advanced Carbon Electrode Materials for Molecular. *Electrochemistry* **2008**, 2646–2687.

(50) Shi, M.; Anson, F. C. Some Consequences of the Significantly Different Mobilities of Hydrophilic and Hydrophobic Metal Complexes in Perfluorosulfonated Ionomer Coatings on Electrodes. *Anal. Chem.* **1997**, *69*, 2653–2660.

(51) Fan, Z.; Harrison, D. J. Permeability of Glucose and Other Neutral Species through Recast Perfluorosulfonated Ionomer Films. *Anal. Chem.* **1992**, *64*, 1304–1311.

(52) Li, F.; Song, J.; Gao, D.; Zhang, Q.; Han, D.; Niu, L. Simple and Rapid Voltammetric Determination of Morphine at Electrochemically Pretreated Glassy Carbon Electrodes. *Talanta* **2009**, *79*, 845–850.

(53) Ensafi, A. A.; Abarghoui, M. M.; Rezaei, B. Simultaneous Determination of Morphine and Codeine Using Pt Nanoparticles Supported on Porous Silicon Flour Modified Ionic Liquid Carbon Paste Electrode. *Sens. Actuators, B* **2015**, *219*, 1–9.

(54) Masui, M.; Sayo, H.; Tsuda, Y. Anodic Oxidation of Amines. Part I. Cyclic Voltammetry of Aliphatic Amines at a Stationary Glassy-Carbon Electrode. *J. Chem. Soc. B* **1968**, No. 973.

(55) Olsen, G. D. Morphine Binding to Human Plasma Proteins. *Clin. Pharmacol. Ther.* **1975**, *17*, 31–35.

(56) Vree, T. B.; Verwey-Van Wissen, C. P. W. G. M. Pharmacokinetics and Metabolism of Codeine in Humans. *Biopharm. Drug Dispos.* **1992**, *13*, 445–460.

(57) Judis, J. Binding of Codeine, Morphine, and Methadone to Human Serum Proteins. *J. Pharm. Sci.* **1977**, *66*, 802–806.

(58) Moaisala, A.; Nasibulin, A. G.; Brown, D. P.; Jiang, H.; Khriachtchev, L.; Kauppinen, E. I. Single-Walled Carbon Nanotube Synthesis Using Ferrocene and Iron Pentacarbonyl in a Laminar Flow Reactor. *Chem. Eng. Sci.* **2006**, *61*, 4393–4402.

(59) Gonzalez, D.; Nasibulin, A. G.; Shandakov, S. D.; Queipo, P.; Jiang, H.; Kauppinen, E. I. Single-Walled Carbon Nanotube Charging during Bundling Process in the Gas Phase. *Phys. Status Solidi B* **2006**, *243*, 3234–3237.